Ecosystem responses in the southern Caribbean Sea to global climate change

Gordon T. Taylor[a,1], Frank E. Muller-Karger[b], Robert C. Thunell[c], Mary I. Scranton[a], Yrene Astor[d], Ramon Varela[d], Luis Troccoli Ghinaglia[e], Laura Lorenzoni[b], Kent A. Fanning[b], Sultan Hameed[a], and Owen Doherty[a]

[a]School of Marine and Atmospheric Sciences, Stony Brook University, Stony Brook, NY 11794; [b]College of Marine Science, University of South Florida, St. Petersburg, FL 33701; [c]Department of Earth and Ocean Sciences, University of South Carolina, Columbia, SC 29208; [d]Estación de Investigaciones Marinas de Margarita, Fundación de la Salle de Ciencias Naturales, Punta de Piedras, Nueva Esparta, Venezuela; and [e]Universidad de Oriente, Boca de Río, Isla de Margarita, Venezuela

Edited by David M. Karl, University of Hawaii, Honolulu, HI, and approved September 20, 2012 (received for review May 4, 2012)

Over the last few decades, rising greenhouse gas emissions have promoted poleward expansion of the large-scale atmospheric Hadley circulation that dominates the Tropics, thereby affecting behavior of the Intertropical Convergence Zone (ITCZ) and North Atlantic Oscillation (NAO). Expression of these changes in tropical marine ecosystems is poorly understood because of sparse observational datasets. We link contemporary ecological changes in the southern Caribbean Sea to global climate change indices. Monthly observations from the CARIACO Ocean Time-Series between 1996 and 2010 document significant decadal scale trends, including a net sea surface temperature (SST) rise of ∼1.0 ± 0.14 °C (±SE), intensified stratification, reduced delivery of upwelled nutrients to surface waters, and diminished phytoplankton bloom intensities evident as overall declines in chlorophyll *a* concentrations (ΔChl*a* = −2.8 ± 0.5%·y^{-1}) and net primary production (ΔNPP = −1.5 ± 0.3%·y^{-1}). Additionally, phytoplankton taxon dominance shifted from diatoms, dinoflagellates, and coccolithophorids to smaller taxa after 2004, whereas mesozooplankton biomass increased and commercial landings of planktivorous sardines collapsed. Collectively, our results reveal an ecological state change in this planktonic system. The weakening trend in Trade Winds (−1.9 ± 0.3%·y^{-1}) and dependent local variables are largely explained by trends in two climatic indices, namely the northward migration of the Azores High pressure center (descending branch of Hadley cell) by 1.12 ± 0.42°N latitude and the northeasterly progression of the ITCZ Atlantic centroid (ascending branch of Hadley cell), the March position of which shifted by about 800 km between 1996 and 2009.

ecosystem state change | oceanography | plankton productivity

Phytoplankton support over 95% of marine food webs and are responsible for about half of the Earth's conversion of CO_2 to biomass through net primary production (NPP) (1). Long-term declines in phytoplankton biomass and production in over 70% of the global ocean have been inferred recently from satellite imagery and century-long shipboard records of water clarity (2, 3). These reports of large-scale changes are at odds with trends directly observed at specific locations within the same ocean domains. For example, the Hawaii Ocean Time-series (HOT) (4) and the Bermuda Atlantic Time-series Study (BATS) (5) report significant increases in phytoplankton production between 1995 and 2005. Changes are attributed to enhanced upward mixing of deepwater nutrients driven by variations in large-scale ocean–atmosphere interactions, such as the El Niño-Southern Oscillation (ENSO), the Pacific Decadal Oscillation (PDO), and the NAO (4, 5). Reviewing six time-series programs worldwide, Chavez et al. (6) report that productivity increased at four stations, remained unchanged at one, and declined at Station CARIACO over the same time period. Sparse observations, methodological differences, regional variations, or simply mismatches in spatial and temporal scaling may account for disparities among local and ocean basin-scale assessments (6). Clearly, reconciling synoptic and local observations is impaired by limited analysis of regional physicochemical and ecological responses to global climatic drivers. Here, we compare temporal trends in ocean productivity, hydrography, and meteorological conditions observed at a station (10.50°N, 64.66°W) located in the marginal southern Caribbean Sea (Fig. 1) with those for global climatic indices over the last 14 y.

Although occupying only ∼8% of the ocean's surface area, continental shelves account for 15–30% of global marine production and >40% of seabed carbon sequestration and are more sensitive to changes in climate and land use than the open ocean (7, 8). Thus, climate-induced changes may be more apparent in marginal seas and have disproportionate impacts on marine ecosystems. Station CARIACO is among the few coastal ocean stations worldwide that has been sampled with at least a monthly sampling frequency for more than a decade (6). The joint Venezuela–United States CARIACO Ocean Time-Series program has collected hydrographic, meteorological, nutrient and carbonate chemistry, phytoplankton standing stock, primary production, sinking flux of particulate matter, and other biogeochemical observations in the anoxic Cariaco Basin since November 1995 (9).

Results and Discussion

From December through May, the southeastern Caribbean experiences upwelling of nutrient-rich subsurface waters as Trade Winds intensify in response to the annual southward migration of the ITCZ (Fig. 1). These zonal winds relax for the remainder of the year, although minor wind-driven secondary upwelling events can occur in July to August (9).The December to May upwelling supports ∼70% of annual NPP (Fig. S1 *A* and *B*). Most NPP occurs in the upper 60 m of the water column (9), where Chl*a* concentrations have averaged 56 mg·m^{-2} during productive periods and are less than 27 mg·m^{-2} otherwise. NPP is usually undetectable below 80 m depth (9).

At Station CARIACO between 1996 and 2010, seasonal peaks in phytoplankton Chl*a* and productivity diminished, particularly after 2003, and annual averages declined significantly ($P < 0.001$). In particular, Chl*a* in the upper 100 m declined at a mean rate of 1.5 ± 0.4 mg Chl*a*·m^{-2}·y^{-1} (Fig. 2 *A* and *B* and Table 1). Annual NPP varied from 370 to 690 g C·m^{-2}, with lower values more common in the 2004–2010 period, and the mean rate of decline was 39 ± 8 mg C·m^{-2}·d^{-1}·y^{-1} (Fig. 2*C* and Table 1). Interpretation of serial datasets is often hampered by autocorrelation. However, autocorrelation analysis of the Chl*a* and NPP time-series yielded coefficients (r) of 0.23 and −0.03, respectively, neither of which was significant ($P > 0.05$). Hence, autocorrelation

Author contributions: G.T.T., F.E.M.-K., R.C.T., M.I.S., Y.A., R.V., and K.A.F. designed research; G.T.T., F.E.M.-K., R.C.T., M.I.S., Y.A., R.V., L.L., K.A.F., and O.D. performed research; Y.A., R.V., L.T.G., L.L., K.A.F., and O.D. contributed reagents/analytic tools; G.T.T., F.E.M.-K., R.C.T., Y.A., R.V., L.T.G., L.L., K.A.F., S.H., and O.D. analyzed data; and G.T.T. wrote the paper.

The authors declare no conflict of interest.

This article is a PNAS Direct Submission.

See Commentary on page 19045.

[1]To whom correspondence should be addressed. E-mail: gordon.taylor@stonybrook.edu.

This article contains supporting information online at www.pnas.org/lookup/suppl/doi:10.1073/pnas.1207514109/-/DCSupplemental.

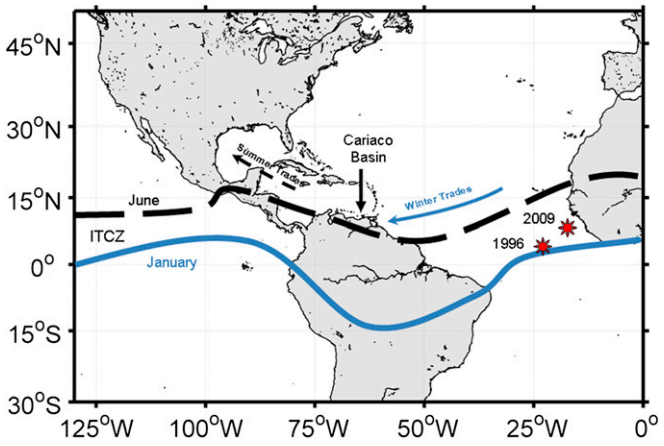

Fig. 1. Geographic location of the CARIACO Ocean Time-Series station (10.50°N, 64.66°W) relative to historical average seasonal positions of the ITCZ. Note that position and intensity of the ITCZ vary among years. Red starbursts indicate March positions of the ITCZ's COA over the Tropical Atlantic in 1996 and 2009.

does not appear to be an issue in the present case. Robustness of reported declines was confirmed by bootstrap resamplings, a procedure that discards randomly selected observations and recalculates rates, correlations, and probabilities with each of the 10,000 iterations to derive consensus values (Figs. S2 and S3). The probability that trends in Chl*a* and NPP are not negative is <<5%, and consensus rates of decline are within 8–9% of regression slopes (Fig. 2 and Figs. S2*A* and S3*A*). Because both Chl*a* and NPP declined at similar rates, production per unit Chl*a* (NPP_{Chla}) varied over similar ranges throughout the entire record, averaging 57 ± 52 mg C·mg $Chla^{-1}\cdot d^{-1}$ (±1 SD), and showed no significant decadal trend ($P > 0.05$) (Fig. S4*A*).

Phaeopigments (*phaeo*) are chlorophyll degradation products that are diagnostic of phytoplankton mortality via herbivory, autolysis, decomposition, viral lysis, and sediment resuspension (10). The distance between our deep-water station and mobile sediments probably eliminates the latter possibility. Therefore, measured *phaeo* is most likely derived from local in situ processes. Particulate *phaeo* concentrations shared similar seasonal patterns with Chl*a* (*phaeo* vs. Chl*a*; $r = 0.87$; $P < 0.0001$) and NPP ($r = 0.56$; $P < 0.0001$). However, proportions of *phaeo* to Chl*a* concentrations (*phaeo*/Chl*a* ratio) were usually lowest in February, highest in May (ANOVA; $P < 0.005$; Fig. S1*C*) and varied inversely with NPP ($r = -0.34$; $P < 0.0001$; $n = 1233$). Variations in *phaeo*/Chl*a* ratios suggest that *phaeo* accumulate relative to Chl*a* and NPP as seasonal blooms succumb to predation and decomposition. Through the entire time-series, *phaeo*/Chl*a* ratios increased at a first-order rate of 2.5 ± 0.33%·y^{-1} (Table 1 and Fig. S4*B*). We recognize that fluorometric measurements of *phaeo* by acidification may be biased by presence of Chl*b* and divinyl-Chl*b* contributed by chlorophytes, prasinophytes, and prochlorophytes (11). However, our limited (5-y) reliable HPLC pigment measurements yielded Chl*b*/Chl*a* ratios varying between 1/10 and 1/3, showing no particular temporal pattern, and suggest that Chl*b*-bearing taxa are not quantitatively dominant at Station CARIACO.

In summary, NPP and Chl*a* inventories declined at first-order rates of 1.7 ± 0.7 and 2.8 ± 0.7%·y^{-1} between 1996 and 2010 (Table 1), whereas the NPP_{Chla} index lacked a discernible trend, and the cumulative *phaeo*/Chl*a* ratio increased by about 42%. Our interpretation of these trends is that photoautotrophic efficiency at the community level has remained relatively stable, whereas the proportional impact of algal mortality has escalated. Collectively, these results suggest that ecosystem structure, function, and perhaps carbon loss terms (via mortality and vertical export) have changed systematically over time.

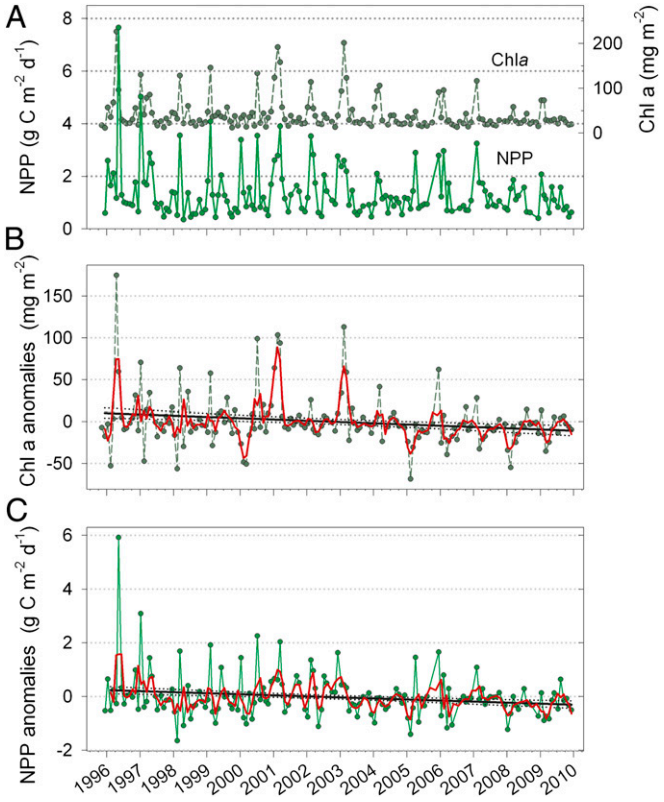

Fig. 2. Time-series of monthly observations of net primary production (NPP) and chlorophyll *a* (Chl*a*) integrated over the upper 100 m (*A*) and deseasonalized data (anomalies) of Chl*a* (*B*) and NPP (*C*). Anomalies were calculated by subtracting monthly means of 14-y record from observations presented in *A*. Red line is three-point running trimmed means (trimean = [minimum + maximum + (2 × median)]/4) used to reduce sensitivity of regressions to outliers. Dotted lines enveloping slopes are 95% confidence intervals.

Shifting Phytoplankton Community Structure, Zooplankton Biomass, and Carbon Export. Monthly taxonomic surveys revealed that from 1996 through 2004 diatoms dominated phytoplankton communities during upwelling, outnumbering dinoflagellates and coccolithophorids by factors of two to three (Fig. 3 *A*–*C*). Starting in 2005, abundances of all three major phytoplankton groups dropped precipitously in the upper 55 m, wherein median inventories between 2005 and 2009 were 50- to 300-fold lower than those from 1996 to 2004 (Fig. 3 *A*–*C*, broken lines). After 2004, diatom and coccolithophorid abundances were essentially equal and fourfold higher than dinoflagellates. Overall declines in cell abundances surpassed those of total Chl*a* by five- to eightfold, implying that phytoplankton not included in our survey (smaller microalgae and various cyanobacteria) replaced the surveyed taxa. Alternatively, larger taxa could have resided in waters deeper than 55 m and escaped detection after 2004, but this interpretation is unsupported by our monthly Chl*a* profiles (www.imars.usf.edu/CAR). Similar taxonomic redistributions have been reported for the BATS station in the Sargasso Sea over this same period (5). Coincident with dramatic drops in large phytoplankton species, commercial landings of the planktivorous sardine (*Sardinella aurita*) on Margarita Island, Venezuela plummeted by 87% (Fig. 3*D*). Collectively, these trends suggest a regime shift in plankton community structure between early and late observations that reverberated throughout the food web. Productivity of *S. aurita* has been shown previously to be very responsive to upwelling intensity and phytoplankton community dynamics (12). However, we caution that the contribution of overexploitation to collapse of this regionally important fishery may also be very important.

Table 1. Rates of change in surface ocean and meteorological and climatic conditions at Station CARIACO and the tropical Atlantic

Variable	Slope* (y^{-1})	SE*	Coefficient of determination* (r^2)	Significance* (P)	First-order constant† k (%·y^{-1})
NPP (mg C·m^{-2}·d^{-1})‡	−39	8.5	0.12	<0.001	−1.7
Chl*a* (mg·m^{-2})‡	−1.5	0.38	0.10	<0.001	−2.8
mg *phaeo* mg Chl*a*$^{-1}$	+0.03	0.004	0.23	<0.001	+2.5
Zooplankton [mg (dry wt)·m^{-2}]	+102	22	0.16	<0.001	+5.0
POC flux (mg C·m^{-2}·d^{-1})§	+1.2	0.50	0.02	<0.02	+1.0
PN flux (mg N·m^{-2}·d^{-1})§	+0.20	0.07	0.02	<0.01	+1.3
$CaCO_3$ flux (mg·m^{-2}·d^{-1})§	+6.6	1.0	0.14	<0.001	+6.0
Opal flux (mg·m^{-2}·d^{-1})§	+3.9	1.0	0.06	<0.001	+2.4
Total mass flux (mg·m^{-2}·d^{-1})§	+22.6	8.2	0.03	<0.007	+2.8
PO_4^{3-} (mmol·m^{-2})‡	−0.66	0.11	0.16	<0.001	−2.4
$Si(OH)_4$ (mmol·m^{-2})‡	−3.7	1.4	0.03	<0.01	−1.2
21 °C isotherm depth (m)	+0.85	0.24	0.10	<0.005	+1.2
SST (°C)	+0.07	0.01	0.14	<0.001	+0.32
Mean density (σ_θ, kg·m^{-3})¶	−0.02	0.003	0.15	<0.001	−0.07
Buoyancy frequency (cycles/h)¶	+0.35	0.05	0.19	<0.001	+0.93
Zonal winds (cm·s^{-1})	−7.6	1.1	0.21	<0.001	−1.9
ITCZ precipitation (mm)	+0.04	0.007	0.16	<0.001	+0.40
ITCZ longitude (°E)	+0.36	0.06	0.19	<0.001	+0.08
ITCZ latitude (°N)	+0.17	0.03	0.18	<0.001	+0.39
Azores High latitude (°N)	+0.08	0.03	0.05	<0.005	+0.20

*Statistics are derived from linear regressions performed on smoothed (three-point running trimmed means) and deseasonalized (anomalies) monthly observations through time (42). Inclusive observation dates are November 8, 1995 through December 8, 2009 for all, except zooplankton (October 9, 2001 through September 6, 2011).

†k is equivalent to linear regression's slope of natural logarithms of actual observations against time and derived from $N = N_0e^{kt}$, where N_0 and N are equal initial and subsequent observations, respectively; t indicates time interval; and k indicates first-order rate of change.

‡0- to 100-m integrals.

§captured in 225-m sediment traps.

¶Weighted means in upper 100 m.

Coincident with shifts in phytoplankton composition and declining standing stocks of phytoplankton and planktivorous sardines, a rise in mesozooplankton (>200 μm) biomass was evident at Station CARIACO (Fig. S5). Even though our mesozooplankton record is shorter because collections did not commence until late 2001, a significantly positive ($P < 0.001$) deseasonalized trend of ~100 ± 22 mg (dry wt)·m^{-2}·y^{-1} or ~5.0 ± 1.7%·y^{-1} is derived from monthly net tows through the upper 200 m (Table 1). Growing mesozooplankton inventories are consistent with the increasing *phaeo*/Chl*a* ratios in the surface water particulates reported above, presumably resulting from fecal pellet contributions. The causes for rising mesozooplankton inventories are uncertain, but relaxation of predation pressures because of planktivorous fish removal and shifting prey composition are both likely to have strong influences.

Plankton community structure and productivity have major effects on sinking fluxes of organic matter and, thereby, influence the efficiency of carbon export, i.e., the "biological carbon pump" (13–15). At Station CARIACO, diatoms historically have been a significant component of sinking fluxes and been responsive to variations in upwelling intensity (16). During the present study, sediment traps deployed at ~225 m measured sinking particulate organic carbon (POC) fluxes varying from ~3 to 240 mg C·m^{-2}·d^{-1}. Similar to *phaeo*/Chl*a* patterns discussed above, median POC fluxes in May were typically threefold higher than those during peak upwelling (December to April). This may illustrate the delayed impacts of zooplankton grazing and phytoplankton bloom collapse on export processes (Fig. S1*D*). In fact, mesozooplankton biomass in the upper 200 m was strongly correlated ($r = 0.51$; $P < 0.001$) with POC fluxes to 425 m but not to 225 m, perhaps reflecting the influence of diel vertical migrations on export dynamics. POC fluxes to 225 m increased by 1.2 ± 0.5 mg C·m^{-2}·y^{-1} between 1996 and 2010 (Fig. S6). Similarly, total settling mass, particulate nitrogen, $CaCO_3$, and biogenic silica (opal) fluxes increased by 2.8 ± 1.0, 1.3 ± 0.5, 6.0 ± 0.9, and 2.4 ± 0.6%·y^{-1}, respectively (Table 1). However, no trends in terrigenous mineral fluxes or C/N ratios of settling material were apparent among years. At the BATS station, export fluxes also have accelerated over this same period (5). Enhanced export fluxes coinciding with declines in diatoms and coccolithophores at the CARIACO and BATS sites are clearly inconsistent with the idea that plankton with heavy mineral frustules/tests preferentially drive vertical export [the "ballast theory" (15)]. In fact, observations from the equatorial Pacific Ocean, Arabian Sea, and Sargasso Sea have all demonstrated that small atestate cells contribute significantly to vertical fluxes, by means of aggregation and consumption/egestion by mesozooplankton (17, 18).

An alternate explanation for opposing trends in NPP and vertical POC flux is that the horizontal transport distance of surface production is proportional to upwelling intensity. Thus, during strong upwelling, POC production processes would be spatially and temporally separated from consumption and export processes as water masses move offshore (19). In fact, we observe that proportional export of NPP to 225 m (e-Ratio) is inversely proportional to NPP (Fig. S6*B*), as shown in studies reviewed in ref. 19. However, all measured upwelling proxies (zonal winds, 21 °C isotherm depth, stratification, nutrients) are very weakly correlated with e-Ratios, explaining ≤10% of the variance in export production (Table S1). Furthermore, sequential Sea-viewing Wide Field-of-view Sensor (SeaWiFS) and Moderate Resolution Imaging Spectroradiometer (MODIS) ocean color satellite images show that our station is generally in the midst of the most productive area. Based on average vertical settling speeds and observed horizontal velocities, we have estimated the statistical collection cone of the moored sediment traps and found that potential aliasing of our trap collections in this area by horizontal advection is negligible (20). We are convinced that biological processes prevail over physical advection in determining apparent dynamics of carbon export to depth at this location, especially because waters below sill depth (90–140 m) exchange very slowly.

Given that mesozooplankton inventories and particulate *phaeo*/Chl*a* ratios have increased despite diminished NPP, we hypothesize that increased export rates at our site are attributable to modified trophic interactions, and possibly higher aggregation

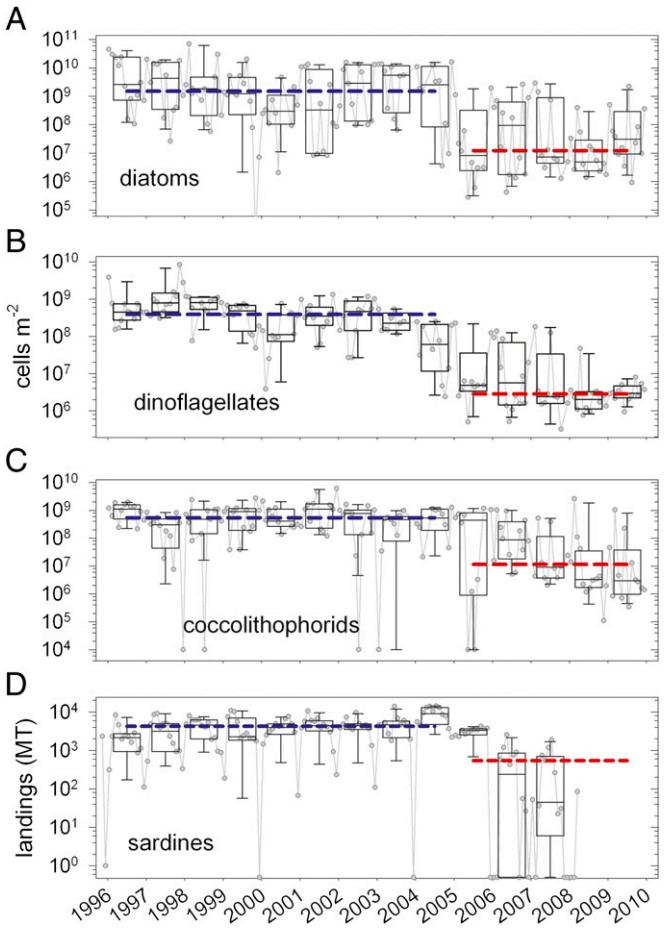

Fig. 3. Shifts in phytoplankton community composition and sardine landings from the southeastern Margarita Island fishery. Monthly observations presented as gray symbols. Box and whisker plots depict binned annual variations in diatom (*A*), dinoflagellate (*B*), coccolithophorid (*C*) inventories integrated over the upper 55 m and sardine fishery landings (*D*) in metric tons. Boxes represent the interquartile range of all observations (25th to 75th percentiles). Internal horizontal lines and whiskers are medians and 10th to 90th percentiles, respectively. Blue and red horizontal lines represent the grand medians of all observations between 1996 and 2004 and between 2005 and 2009, respectively. Data in early and late bins are significantly different in all cases (ANOVA; $P < 0.001$). [Fishery data are courtesy of L. W. Gonzáles (Universidad de Oriente, Boca de Río, Isla de Margarita, Venezuela); zero values artificially set at 0.5 for plotting purposes.)

frequencies, all induced by community structure shifts. Observations such as these from Station CARIACO and far-ranging biomes challenge the prediction by Bopp et al. (21) that selection for smaller phytoplankton taxa by a warming ocean necessarily lowers carbon sequestration efficiency of the "biological carbon pump."

Environmental Forcing Alters Upper Ocean Ecology. Changing nutrient supply to surface waters is the most likely proximal cause for declining plankton productivity at Station CARIACO. For example, inventories of PO_4^{3-} in the upper 100 m varied seasonally between 5 and 70 mmol·m^{-2} over the last 14 y; building from December through March, and exhibiting secondary maxima in July (Fig. S7*A*). However, PO_4^{3-} in the upper 100 m declined on average by 0.7 ± 0.1 mmol·m^{-2}·y^{-1} or 2.4%·y^{-1} in our dataset (Table 1 and Fig. S7 *B* and *C*). Silicate inventories (Si[OH]$_4$) showed similar seasonal and longer term trends, declining at rates of 3.7 ± 1.4 mmol·m^{-2}·y^{-1} or 1.2%·y^{-1} (Table 1 and Fig. S7*D*). Although seasonal trends for nitrate resembled those of PO_4^{3-}, dissolved inorganic nitrogen species (NO_3^-, NO_2^-, NH_4^+) generally exhibited no significant long-term trend, probably because of nitrogen's more complex cycling in oxygen-depleted water columns (i.e., N fixation, nitrification, denitrification, anammox, etc.) (22).

Declining PO_4^{3-} and Si[OH]$_4$ in surface waters coincided with indicators of weakened upwelling. Seasonal shoaling of the 21 °C isotherm is diagnostic of upwelling of nutrient-rich waters in this region. In fact, deseasonalized variations in shallow PO_4^{3-} inventories and the 21 °C isotherm depth were highly correlated ($r = -0.90$; $P << 0.001$; Table S2) as were Si[OH]$_4$ inventories ($r = -0.49$; $P < 0.001$). Whereas the seasonal cycle remained intact throughout the record, the amplitude and duration of the 21 °C isotherm's upward excursions decreased in the latter portion of the record (Fig. S8*A*). The mean position of the 21 °C isotherm deepened by 0.85 ± 0.24 m·y^{-1}, a descent equivalent to 1.2%·y^{-1} (Table 1 and Fig. S8*B*). Mean temperatures in the upper 4 m [sea surface temperature (SST)] at Station CARIACO have systematically risen since 1996 by 0.07 ± 0.01 °C·y^{-1} or 0.3%·y^{-1} (Table 1 and Fig. S8*C*). This warming trend was primarily driven by rising temperature minima during the upwelling season (Fig. S8*D*). Mean water density (σ_θ) in the upper 100 m has declined significantly by 0.02 ± 0.003 kg·m^{-3}·y^{-1} or 0.07%·y^{-1}, resulting from warmer SSTs and less intense upwelling (Table 1). These processes amplified density differences with underlying waters, thereby enhancing stratification, which is manifested by monthly means of the Brunt–Väisälä buoyancy frequency increasing at a rate of 0.35 ± 0.05 cycles·h^{-1}·y^{-1} or 0.93%·y^{-1} in the upper 100 m (Table 1 and Fig. S9). Clearly, hydrographic conditions at the CARIACO site have changed to a state less favorable for upward nutrient transport and consequently less supportive of primary producers.

Local Conditions Linked to Global Climatic Changes. Zonal wind stress ($-u$, easterly Trade Winds) across the southern Caribbean Sea drives near-shore upwelling of nutrient-rich waters by Ekman transport. Observations from Margarita Island show that duration of sustained zonal winds exceeding 6 m·s^{-1} and peak monthly average speeds have diminished over our 14-y observation period (Fig. S10*A*). Mean upwelling-favorable winds have weakened by 7.6 ± 1.1 cm·s^{-1}·y^{-1} or ~1.9%·y^{-1} (Table 1 and Fig. S10*B*). Our observations are consistent with a recent global survey of satellite data collected from 1991 to 2008, showing declining mean wind speeds and wave heights in the southern Caribbean, while increasing elsewhere in the world's ocean (23). Two decadal-scale regimes are evident: strong Trade Winds in 1996–2003 and weaker winds in 2004–2010. Deseasonalized trends in zonal winds unmistakably influence upwelling intensity, SST, density and stability of surface waters, [PO_4^{3-}], NPP, and Chl*a* at Station CARIACO, explaining 22–64% of their variance (r^2) (Table S2).

How, then, might global climate variability drive local trends in Trade Wind behavior? The NAO index is well correlated with weather patterns in Europe and Africa, and oceanographic changes in the western Sargasso Sea (5, 24). It is a climatic teleconnection defined as the difference in sea level pressure (SLP) anomalies between the Azores High and the Icelandic Low. We found only modest correlations between deseasonalized variations in the NAO index and SST observations ($r^2 = 26\%$ of variance; $P < 0.10$) at Station CARIACO (Table S3). In contrast, variations in SLP and the latitudinal position of the Azores High (descending Hadley cell branch) among years explained as much as 56% of variances in SST, zonal winds, and upwelling intensity at our station. Our analysis illustrates that the Azores High has systematically migrated northward at 0.08 ± 0.03°N·y^{-1} since 1996, apparently affecting conditions in the Caribbean somehow (Fig. 4*A* and Table 1).

The ENSO climatic teleconnection affects a major portion of the Pacific Ocean at low latitudes and reputedly influences wind, SST, and precipitation patterns in the Caribbean and the Americas (25, 26). However, none of the well-known ENSO indices, including the multivariate ENSO MEI index, correlates with measurements at Station CARIACO, other than local pre-

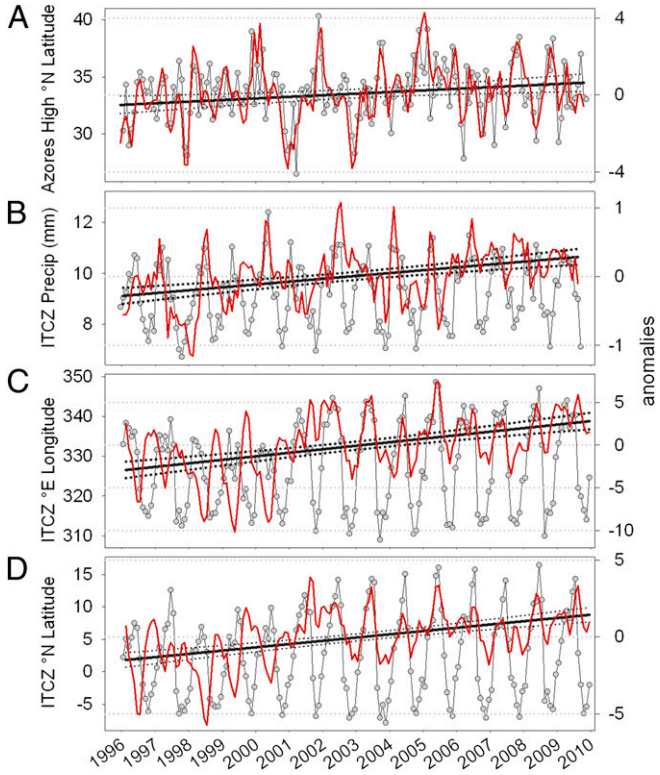

Fig. 4. Temporal variations in the indices for the Azores High pressure center (*A*) and ITCZ (*B–D*) during the CARIACO time-series. (*A*) Monthly variations in the latitudinal position of the Azores High pressure COA. (*B*) Monthly variations in the South American precipitation index. Monthly variations in the longitudinal (*C*) and latitudinal (*D*) positions of the Tropical Atlantic ITCZ's COA. Circles indicate mean monthly observations, and red lines are three-point running trimeans of computed anomalies used for regression analysis. Dotted lines enveloping slopes are 95% confidence intervals.

cipitation. Variations in Caribbean conditions have been reported to lag approximately 1 y behind ENSO, and the response strength to vary on decadal time scales (27). By lagging local anomalies 1 y behind the MEI (ENSO MEI-1), 24–36% of the variance in SST, zonal winds, surface water density and stability, NPP, and Chl*a* at Station CARIACO, as well the NAO and Azores SLP indices, were explained by ENSO variations (Tables S2 and S3).

Position and strength of the equatorial Trade Wind convergence control SLP, precipitation patterns, and dynamics of the ascending portions of the Hadley circulation cell (the ITCZ). We used the National Center for Environmental Prediction (NCEP) Reanalysis dataset to identify the ITCZ's location and strength using precipitation and wind convergence fields. The ITCZ over South America migrates annually from about 10–15°N in July to August to >15°S latitude in December to January and then returns (Fig. 1). Local winds over the Cariaco Basin are weakest and precipitation highest when the ITCZ is in its northernmost position. Winds strengthen, whereas rainfall abates, as the ITCZ migrates southward annually.

Between 1996 and 2010, the ITCZ precipitation index over South America systematically increased (0.04 ± 0.007 mm·y^{-1}) (Fig. 4*B* and Table 1), suggesting a strengthening of the ITCZ. Zonal position of its centroid was negatively correlated with local precipitation and winds, as well as the ENSO MEI (Table S3). Although we did not detect changes in the seasonal cycle of atmospheric convergence intensity of the Tropical Atlantic ITCZ, expansions of seasonal zonal and meridional excursions were evident (Fig. 4 *C* and *D*). During our study, mean position of the centroid of this ITCZ index migrated $0.36 \pm 0.06°$ eastward and $0.17 \pm 0.03°$ northward annually (Table 1). Between 1996 and 2009 in the month of March, when Trade Winds were consistently strong (Fig. S10*A*), the ITCZ centroid is estimated to have migrated ~800 km to the northeast over the Tropical Atlantic (Fig. 1).

These analyses link decadal trends in the ITCZ and the Azores High to present-day marine ecosystem state changes in the southern Caribbean. Our findings are consistent with Cariaco Basin's paleoceanographic record showing that climate in Central and South America over the last ~14,000 y responded to variations in the mean position of the ITCZ (28). Based on lake sediment proxies in the tropical Pacific, Sachs et al. (29) concluded that the ITCZ shifted southward during climatic cooling periods and northward during warming periods over the past millennium. In the 1960s, the ITCZ occupied a northeasterly position and a more southwesterly position during the 1980s and 1990s, putatively causing changes in weather patterns over northern Africa and in Europe (30). Our results show that from 1996 onward, the ITCZ has been on a northeasterly progression over the Atlantic, consistent with a history of climatic warming. Several recent studies have shown that the ITCZ's driver, Hadley cell circulation, has shifted and expanded in recent decades (31–36). Temporal trends in atmospheric ozone distributions suggest that the tropical belt grew at a rate of 1° latitude per decade between 1979 and 2003 (32). Other proxies suggest that the Hadley cell has been widening somewhere between ~0.8 and 3° latitude per decade over this period (31, 33, 34). The descending branch of the Hadley cell forms the boundary between the tropical belt and subtropical arid zone, controlling the Azores High's position. The Intergovernmental Panel on Climate Change (IPCC) concluded that the Hadley cell will continue to expand and spread subtropical deserts poleward under present greenhouse gas emission scenarios (35–37).

Our analyses are consistent with cited studies of the Azores High and ITCZ (Fig. 4) and IPCC predictions and suggest that Hadley cell dynamics have led to changes in the Trade Winds in the southern Caribbean. These, in turn, have affected the oceanography, carbon sequestration, and ecosystem structure/function, particularly plankton productivity (Figs. 2 and 3), with possible socioeconomic consequences. We caution that our decadal-scale observations do not permit unequivocal resolution of whether these are manifestations of unidirectional trends driven by anthropogenic climate change or whether they simply reflect low-frequency natural cycles, such as those driving the Atlantic Multidecadal Oscillation.

Conclusions

Biogeochemical measurements at the CARIACO Ocean Time-Series document a decadal decline in plankton productivity. This is an expression of a significant marine ecosystem state change driven by diminished upwelling, warming surface waters, and increased stratification, all contributing to waning nutrient supplies. Other ecosystem responses include altered plankton community structure and function and enhanced export flux of organic matter to deeper waters. We find compelling evidence that contemporary decadal scale shifts in the ITCZ and Azores High positions are linked to slackening Trade Winds that drive coastal upwelling in this region. Our results underscore the value of intensive multidisciplinary time-series studies to understand local effects of climatic changes on the behavior of marine ecosystems, including living marine resources.

Materials and Methods

Data. Sampling and processing protocols for hydrography, NPP, Chla, *phaeo*, nutrient concentrations, and sediment trap deployment and processing appear in Muller-Karger et al. (8). These data are available from www.imars.usf.edu/CAR, the National Oceanographic Data Center (NODC) (www.nodc.noaa.gov), and the Biological and Chemical Oceanography Data Management Office (BCO-DMO) (http://bco-dmo.org/data). From late 1995 to early 1998, nutrient data were provided by William Senior (Universidad de Oriente, Cumana, Venezuela) and by Dr. K. Fanning (University of South Florida, St. Petersburg, FL) from mid-1997 to the present. Samples from eight cruises were analyzed by both laboratories; PO_4^{3-} and $Si[OH]_4$ data agreed very well (±5%), but NO_x and NH_4^+ did not. Therefore, the entire PO_4^{3-} and $Si[OH]_4$ dataset and only the USF NO_x and NH_4^+ dataset were used here. Wind data were obtained from Santiago Mariño Airport (10°54′N, 63°57.60′W) and

the Fundación la Salle's Estación de Investigaciones Marinas (EDIMAR) at Punta de Piedras, Margarita Island (10°54′N, 64°12′W). Meteorological stations are only 26 km apart on Margarita Island, and both are ∼80 km northeast of Station CARIACO. Phytoplankton enumeration was conducted on water samples (500 mL) collected by Niskin bottles at depths of 1, 7, 15, 25, 35, 55 m and fixed with 5% sodium tetraborate-buffered formaldehyde (final concentration). Quantitative analyses were performed using settling chambers and an inverted microscope according the Utermöhl method (38). Mesozooplankton were captured by oblique tows of paired 200- and 500-μm bongo nets (diameter, 60 cm), equipped with TSK flow meters, and lowered to 200 m at Station CARIACO. Care was taken to tow for the same duration between 0900 and 1030 hours in all cases, and cable angle was monitored to assess net depths and adjust the ship's speed as necessary. Samples were quantitatively split and zooplankton dry weight subsamples were captured on tared filters, rinsed with deionized water, dried at 65 °C for 48 h and weighed. Volumetric masses (milligram per cubic meter) were multiplied by the depth of integration (200 m) to yield grams dry weight per square meter.

To gauge ITCZ changes relevant to Cariaco Basin data, we developed ITCZ indices over South America (20°S to 5°N and 290°W to 320°W) and the Tropical Atlantic (15°S to 20°N and 300°W to 357.5°W) as area-weighted precipitation and convergence, using the precipitation intensity and negative divergence of horizontal winds, respectively. We calculate ITCZ indices using the previously described center of action (COA) approach (39). The NCEP Reanalysis (40) was the source of data for NAO (www.cgd.ucar.edu/cas/jhurrell/ indices.html), Azores High, and ITCZ analyses. Precipitation intensities were obtained from Global Precipitation Climatology Project (41). In all cases except the NAO, derived data were obtained from the National Oceanic and Atmospheric Administration/Office of Oceanic and Atmospheric Research/Earth System Research Laboratory Physical Sciences Division (NOAA/OAR/ESRL PSD) (www.esrl.noaa.gov/psd). Monthly multivariate ENSO indices (ENSO MEI) were obtained from www.esrl.noaa.gov/psd/enso/mei (Courtesy of K. Wolter, NOAA ESRL).

Analyses. To test for trends throughout our records, seasonal cycles were removed from each variable by subtracting monthly means for entire dataset from individual observations to generate anomalies. These deseasonalized data were analyzed by linear regressions performed on smoothed curves generated from three-point running trimmed means of the anomalies (trimean = [minimum + maximum + (2 × median)]/4) (42). Running trimeans reduce regression sensitivity to outliers by doubling the weight of median values. Contour plots were generated using Ocean Data View (http://odv.awi.de). Linear regressions, ANOVA, and Pearson product moment correlations were performed using SigmaPlot/SigmaStat package (version 12; Systat Software).

ACKNOWLEDGMENTS. We thank the captain and crew of the B/O Hermano Gines and the staff of Estación de Investigaciones Marinas de Margarita, Fundación de la Salle de Ciencias Naturales for their field assistance. We also thank the many students, postdocs, and technicians who have participated in this project. We thank L. W. González (Universidad de Oriente) for providing commercial sardine landing data. This research was supported by National Science Foundation (NSF) Grants OCE-0326175 and OCE-0752014 (to M.I.S. and G.T.T.) and OCE-9216626, OCE-9729284, OCE-0118566, OCE-0326268, OCE-0752139, OCE-0963028, and OCE-0326268 (to F.E.M.-K. and R.C.T.) and Venezuela Fondo Nacional de Ciencia, Tecnología e Innovación (FONACIT) Grants 96280221 and 2000001702 (to R.V.). This work is School of Marine and Atmospheric Sciences contribution no. 1413.

1. Field CB, Behrenfeld MJ, Randerson JT, Falkowski P (1998) Primary production of the biosphere: Integrating terrestrial and oceanic components. *Science* 281(5374): 237–240.
2. Behrenfeld MJ, et al. (2006) Climate-driven trends in contemporary ocean productivity. *Nature* 444(7120):752–755.
3. Boyce DG, Lewis MR, Worm B (2010) Global phytoplankton decline over the past century. *Nature* 466(7306):591–596.
4. Corno G, et al. (2007) Impact of climate forcing on ecosystem processes in the North Pacific Subtropical Gyre. *J Geophys Res* 112(C4):C04021.
5. Lomas MW, et al. (2010) Increased ocean carbon export in the Sargasso Sea linked to climate variability is countered by its enhanced mesopelagic attenuation. *Biogeosciences* 7(1):57–70.
6. Chavez FP, Messié M, Pennington JT (2011) Marine primary production in relation to climate variability and change. *Annu Rev Mar Sci* 3:227–260.
7. Yool A, Fashman MJR (2001) An examination of the 'continental shelf pump' in an open ocean general circulation model. *Global Biogeochem Cycles* 15(4):831–844.
8. Muller-Karger FE, et al. (2005) The importance of continental margins in the global carbon cycle. *Geophys Res Lett* 32(1):L01602.
9. Muller-Karger F, et al. (2001) Annual cycle of primary production in the Cariaco Basin: Response to upwelling and implications for vertical export. *J Geophys Res* 106(C3): 4527–4542.
10. Lorenzen CJ (1967) Vertical distribution of chlorophyll and phaeo-pigments: Baja California. *Deep Sea Res* 14(6):735–745.
11. Welschmeyer NA (1994) Fluorometric analysis of chlorophyll *a* in the presence of chlorophyll *b* and phaeopigments. *Limnol Oceanogr* 39(8):1985–1992.
12. Gonzáles LW, Eslava N, Gómez E (2007) Parámetros poblacionales de al sardina (*Sardinella aurita*) del sureste de la Isla de Margarita, Venezuela. *Boletín del Centro de Investigaciones Biológicas* 41(4):457–470.
13. Michaels AF, Silver MW (1988) Primary production, sinking fluxes and the microbial food web. *Deep Sea Res* 35(4):473–490.
14. Taylor GT, Karl DM (1991) Vertical fluxes of biogenic particles and associated biota in the eastern North Pacific: Implications for biogeochemical cycling and productivity. *Global Biogeochem Cycles* 5(3):289–303.
15. Armstrong RA, et al. (2002) A new, mechanistic model for organic carbon fluxes in the ocean based on the quantitative association of POC with ballast minerals. *Deep Sea Res Part II Top Stud Oceanogr* 49(1-3):219–236.
16. Romero OE, et al. (2009) Seasonal and interannual dynamics in diatom production in the Cariaco Basin, Venezuela. *Deep Sea Res* 56(4):571–581.
17. Richardson TL, Jackson GA (2007) Small phytoplankton and carbon export from the surface ocean. *Science* 315(5813):838–840.
18. Lomas ML, Moran SB (2011) Evidence for aggregation and export of cyanobacteria and nano-eukaryotes from the Sargasso Sea euphotic zone. *Biogeosciences* 8(1): 203–216.
19. Pennington JT, et al. (2009) The Northern and Central California coastal upwelling system. *Carbon and Nutrient Fluxes in Continental Margins: A Global Synthesis. JGOFS Continental Margins Task Team (CMTT)*, eds Liu KK, et al. (Springer-Verlag, Berlin, Heidelberg), pp 29–44.
20. Muller-Karger FE, et al. (2010) The CARIACO oceanographic time-series. *Carbon and Nutrient Fluxes in Continental Margins: A Global Synthesis. JGOFS Continental Margins Task Team (CMTT)*, eds Liu KK, et al. (Springer-Verlag, Berlin, Heidelberg), pp 454–464.
21. Bopp L, et al. (2005) Response of diatoms distribution to global warming and potential implications: A global model study. *Geophys Res Lett* 32(19):L19606.
22. Zehr JP (2009) New twist on nitrogen cycling in oceanic oxygen minimum zones. *Proc Natl Acad Sci USA* 106(12):4575–4576.
23. Young IR, Zieger S, Babanin AV (2011) Global trends in wind speed and wave height. *Science* 332(6028):451–455.
24. Hurrell JW (1995) Decadal trends in the north Atlantic oscillation: Regional temperatures and precipitation. *Science* 269(5224):676–679.
25. Enfield DA, Mayer DA (1997) Tropical Atlantic sea surface temperature variability and its relation to El Niño-Southern Oscillation. *J Geophys Res* 102(C1):929–945.
26. Alexander MA, et al. (2002) The atmospheric bridge: The influence of ENSO teleconnections on air–sea interaction over the global oceans. *J Clim* 15(16):2205–2231.
27. Giannini A, Cane MA, Kushnir Y (2001) Interdecadal changes in the ENSO teleconnection to the Caribbean region and the North Atlantic Oscillation. *J Clim* 14(13): 2867–2879.
28. Haug GH, Hughen KA, Sigman DM, Peterson LC, Röhl U (2001) Southward migration of the intertropical convergence zone through the Holocene. *Science* 293(5533):1304–1308.
29. Sachs JP, et al. (2009) Southward movement of the Intertropical Convergence Zone AD 1400-1850. *Nat Geosci* 2(7):519–525.
30. Kapala A, Maè Chel H, Flohn H (1998) Behaviour of the centres of action above the Atlantic since 1881. Part II: Associations with regional climate anomalies. *Int J Climatol* 18(1):23–26.
31. Seidel DJ, Randel RJ (2007) Recent widening of the tropical belt: Evidence from tropopause observations. *J Geophys Res* 112(D20):D20113.
32. Hudson RD, et al. (2006) The total ozone field separated into meteorological regimes – part II: Northern Hemisphere mid-latitude total ozone trends. *Atmos Chem Phys* 6:5183–5191.
33. Fu Q, Johanson CM, Wallace JM, Reichler T (2006) Enhanced mid-latitude tropospheric warming in satellite measurements. *Science* 312(5777):1179.
34. Hu Y, Fu Q (2007) Observed poleward expansion of the Hadley circulation since 1979. *Atmos Chem Phys* 7(19):5229–5236.
35. Previdi M, Liepert BG (2007) Annular Modes and Hadley cell expansion under global warming. *Geophys Res Lett* 34(22):L22701.
36. Lu J, Vecchi GA, Reichler T (2007) Expansion of the Hadley cell under global warming. *Geophys Res Lett* 34(6):L06805.
37. Meehl GA, et al. (2007) *The Physical Science Basis. Contribution of Working Group I to the Fourth Assessment Report of the Intergovernmental Panel on Climate Change*, eds Solomon S, et al. (Cambridge University Press, Cambridge, UK).
38. Hasle GR (1978) The inverted microscope method. *Phytoplankton Manual*, ed Sournia A [Scientific Committee on Oceanic Research–United Nations Educational, Scientific and Cultural Organization (SCOR-UNESCO), Paris], pp. 88–96.
39. Doherty OM, Riemer N, Hameed S (2008) Saharan mineral dust transport into the Caribbean: Observed atmospheric controls and trends. *J Geophys Res* 113(D7):D07211.
40. Kalnay E, et al. (1996) The NCEP/NCAR reanalysis 40-year project. *Bull Am Meteorol Soc* 77(3):437–471.
41. Adler RF, et al. (2003) The Version 2 Global Precipitation Climatology Project (GPCP) monthly precipitation analysis (1979-Present). *J Hydrometeorol* 4(6):1147–1167.
42. Wilks DS (2006) *Statistical Methods in the Atmospheric Sciences* (Elsevier, Boston), 627 pp.